Oil Shale, 2025, Vol. 42, No. 2, pp. 208–226
doi: https://doi.org/10.3176/oil.2025.2.04 ISSN 0208-189X

Research on deformation monitoring system of in situ heater in oil shale wells

Hao Yang[a,b,c]*, Tianyu Sun[c], Hao Zeng[a,b], Junshan Ren[c]

[a] State Key Laboratory of Shale Oil and Gas Enrichment Mechanisms and Effective Development, 197 Baisha Road, Changping District, Beijing 100083, China
[b] State Center for Research and Development of Oil Shale Exploitation, 197 Baisha Road, Changping District, Beijing 100083, China
[c] School of Engineering and Technology, China University of Geosciences (Beijing), 29 Xueyuan Road, Haidian District, Beijing 100083, China

Received 11 August 2024, accepted 9 April 2025, available online 11 April 2025

Abstract. *The in situ heater, a pivotal component for oil shale heating, is prone to deformation at underground temperatures of up to 450 °C. While lab experiments with optical fiber technology can monitor deformation at temperatures up to 1100 °C, low-pressure tolerance and complex manufacturing hinder its underground application. Current downhole monitoring systems are limited to 300 °C for temperature and 100 °C for deformation, which are insufficient for oil shale conditions. A dedicated online monitoring system for in situ heaters is still lacking. Leveraging the precision and reliability of linear variable differential transformer (LVDT) technology, we designed a real-time deformation monitoring system. Indoor simulations mimicking oil shale environments indicate LVDT's capability of monitoring up to 480 °C. The system mounts an LVDT unit, encapsulated in vacuum insulation, onto heaters, and then inserts them into horizontal sections via tubing. This design offers a valuable reference for the design and monitoring of in situ heaters in oil shale wells.*

Keywords: *oil shale, deformation, high temperature, monitoring system, in situ, heater.*

1. Introduction

With the continuous exploitation of oil and gas resources, the reserves of conventional oil and gas have declined significantly, making the search for diversified and suitable alternative energy sources an important strategic direction for national energy development. China is rich in oil shale reserves,

* Corresponding author, yanghcugb@163.com

which are widely distributed, totaling about 7.2 × 10^{11} tons [1–4]. Geological exploration results show that China's oil shale has moderate oil content, with a relatively small proportion of high-maturity deposits, posing difficulties in mining.

Oil shale mining technology can be divided into surface distillation and underground in situ mining. The main technical method of surface distillation is similar to existing coal mining technologies. Oil shale is extracted through open-pit or underground mining, transferred to the surface, and then subjected to grinding and screening before the dry distillation process, where shale oil is obtained. Although this technology is relatively mature and the process is simple, there are inevitably problems, such as low utilization rates, small-scale operations, high costs, and significant environmental pollution, including waste gas, waste water, and dust emissions. Additionally, dry distillation produces large amounts of waste residue, while the product coke and semi-coke are not easy to recycle, imposing significant limitations on this method.

In contrast, underground in situ mining technology is suitable for deep oil shale deposits and has the advantages of high mining efficiency, good product quality, space savings, and minimal environmental pollution, making it a focus of various countries. Heating oil shale is a critical aspect of in situ mining, and the heating methods can be divided into four types: electric conduction heating, fluid convection heating, radiation heating, and combustion heating [5–7]. Currently, many oil shale wells in China employ near-critical water in situ extraction technology. This technique utilizes the principle of convective heating by injecting water into the oil shale reservoir through an injection well. A heating device placed downhole heats the water until it reaches a near-critical state, allowing it to transfer heat to the reservoir. Since near-critical water reacts with organic matter, it facilitates the cracking of the organic material. The resulting cracked organic matter is then extracted using the inherent properties of near-critical water, with oil-water separation occurring on the surface to ultimately obtain shale oil [8].

A large amount of organic matter in oil shale cannot be directly extracted and requires retorting to obtain crude oil. As shown in Figure 1, in situ mining technology is a commonly used technique for oil shale mining [9, 10]. When the temperature reaches 450–600 °C, the organic matter begins to rapidly crack into oil and gas, which are then extracted through specific processes [11]. Heaters, as key equipment in the in situ mining of oil shale, operate in high-temperature and high-pressure environments for a long time. This makes them prone to deformation, which affects their mechanical properties and stability.

Through deformation monitoring, tiny changes in the shape of heaters can be detected promptly, enabling the prediction and prevention of potential failures, and avoiding production interruptions or safety accidents caused by sudden equipment malfunctions. Extensive research has been conducted on deformation monitoring methods and systems both domestically and

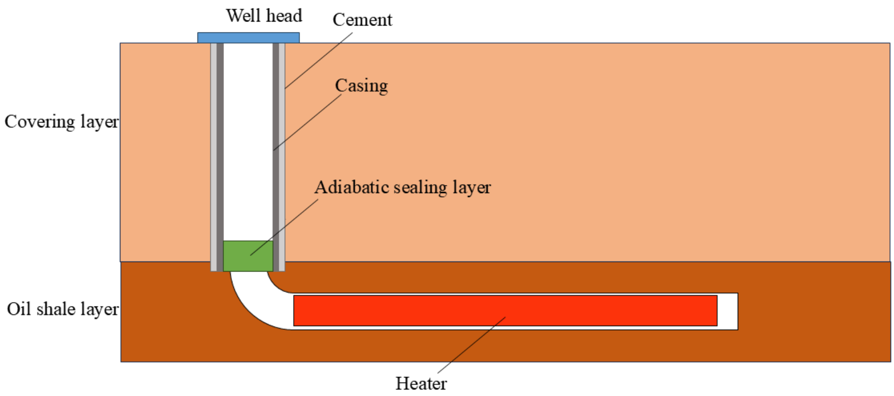

Fig. 1. Schematic diagram of in situ heating of oil shale.

internationally, mainly based on strain [12–14], vibration [15], and vision [16–18]. Strain measurement is widely used because it does not involve external excitation, and its results can directly reflect the operating state of the structure.

For deformation monitoring under high-temperature conditions, the digital image correlation (DIC) method is a typical non-contact deformation measurement technique that can effectively measure surface deformations. Chen et al. [19] used monochromatic light digital image technology to measure the expansion deformation of specimens at 1100 °C. Berke et al. [20] employed ultraviolet digital image technology to measure the deformation of specimens at 1125 °C after filtering out their spontaneous visible light. Based on this, Qiao et al. [21] used a 3D-DIC system to measure the expansion deformation of specimens within the temperature range of 25–2000 °C, significantly improving the upper-temperature limit of measurable deformation. Although vision-based deformation methods have the advantages of reduced workload and high reliability, they mainly involve image acquisition and tracking, making them difficult to implement underground or in wells. Furthermore, the testing equipment itself is not resistant to high temperatures. Xia et al. [22] proposed and studied a photonic crystal fiber (PCF) Fabry-Perot (F-P) sensor for large strain measurements at high temperatures. This sensor can accurately detect a large mechanically induced strain of 9436.66 με at temperatures as high as 1000 °C. Li et al. [23] developed an all-fiber F-P high-temperature strain sensor that can withstand temperatures up to 1100 °C; however, it operates at relatively low pressures. Gao et al. [24] summarized the performance of high-temperature fiber Fabry-Perot pressure sensors made from sapphire and silicon carbide after encapsulation, which can be used for pressure measurement in environments exceeding 800 °C. While these laboratory experiments show that such sensors can be used under high-temperature conditions, they operate at low pressures, and the cost of optical fibers is high. To date, no sensors have been reported for monitoring the in situ heating of oil shale.

Currently, research on downhole monitoring systems for oil wells mainly focuses on temperature and pressure monitoring. Yu et al. [25] studied an optical fiber F-P cavity pressure sensor that can measure pressures up to 30 MPa at 300 °C. Li et al. [26] developed a high-precision fiber Bragg grating temperature sensor that can measure temperatures up to 175 °C under 100 MPa. Yang et al. [27] developed a high-precision fiber-optic temperature and pressure sensor that meets the monitoring requirements of production wells at 100 °C. At present, there is limited research on downhole deformation monitoring, with studies mainly focusing on casings. Wang [28] explored a fiber-optic sensing technology for monitoring deformation in oil and water well casings, capable of monitoring deformations in wells at 100 °C. Most downhole monitoring systems are designed for ordinary oil wells, and there is no relevant literature on deformation monitoring of oil shale downhole heaters.

The linear variable differential transformer (LVDT) is a precise linear position sensor capable of measuring position within a wide range, making it a promising and valuable tool for deformation measurement. Chen et al. [29] studied an LVDT test system for measuring radial deformation, capable of measuring radial strains as low as 0.0001%. Mayunga et al. [30] combined GPS with LVDT to conduct dynamic deformation monitoring of the Lausanne Bridge, effectively measuring the bridge's deformation. Gruber et al. [31] studied the effects of temperature on different plunger materials in harsh environments. Currently, LVDTs are widely used in deformation monitoring due to their high precision. However, there is no relevant research on their application under high-temperature conditions.

During in situ heating, the downhole temperature of oil shale reaches 450–600 °C, and current downhole monitoring systems cannot meet this requirement. LVDTs offer good stability and do not require direct contact with the measured object, allowing them to operate reliably in harsh environments such as high temperatures, high pressures, and high humidity [32, 33]. However, to date, LVDTs have not been used for real-time monitoring of downhole deformation. This paper designs a real-time deformation monitoring system suitable for in situ heaters in oil shale wells.

2. Experimental method

2.1. Principle

The two ends of the sensor are fixed to both ends of the object to be measured. As shown in Figure 2, when the temperature rises, the object expands and undergoes axial deformation. This causes the fixed end above the sensor to move upwards, driving the magnetic core to move upwards as well, cutting through the magnetic induction coil and generating an electrical signal.

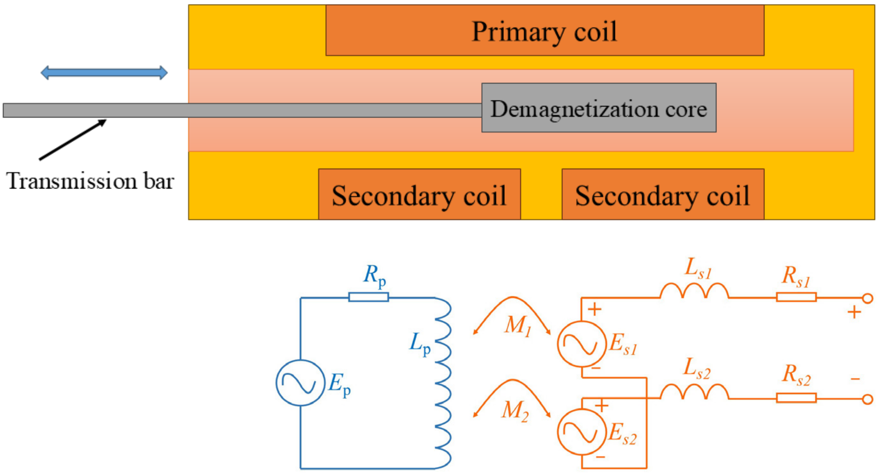

Fig. 2. Sensor working principle. Abbreviations: R_p – resistance of the primary coil, L_p – inductance of the primary coil, E_p – excitation voltage applied to the primary coil, L_{s1} – inductance of the first secondary coil, L_{s1} – inductance of the second secondary coil, E_{s1} – induced voltage in the first secondary coil, E_{s2} – induced voltage in the second secondary coil, R_{s1} – resistance of the first secondary coil, R_{s1} – resistance of the second secondary coil.

The electrical signal is transmitted to the receiving device through the connecting cable, and the deformation of the measured object is determined by calculating the change in electromotive force using software. The LVDT boasts high measurement accuracy, enabling it to measure subtle deformations in oil shale in situ heaters. Its non-contact measurement method ensures long-term use without easy damage.

2.2. Deformation monitoring experiment

To assess the monitoring capabilities of the designed sensor for deformation, an experimental setup was constructed, as illustrated in Figure 3. This system encompasses a triaxial confining pressure chamber, a hydraulic servo controller, a sensor, and other vital components. A columnar core is positioned within a high-temperature and high-pressure kettle (Fig. 4), which is interfaced with a constant pressure pump via a metal pipe to maintain stable confining pressure. The kettle is also connected to a low-temperature circulating water bath system through a separate channel for cooling purposes. Subsequently, the kettle is insulated with a heat insulator and heated by a dedicated heating device. A thermocouple, installed through the insulation sleeve and a reserved port in the kettle, continuously monitors the internal temperature of the core in real time (Fig. 5). The hydraulic servo controller supplies the necessary pressure, applying both axial and confining pressures independently through the triaxial confining chamber to mimic downhole conditions. When the core undergoes expansion or compression, resulting in axial displacement of the upper fixation device on the kettle, the electrical signal from the LVDT sensor is transmitted via a cable to a receiving device. This signal is then processed by software to calculate the deformation, enabling real-time monitoring of the core's deformation (Fig. 6). During the experimental trials, the temperature (ranging from 25 to 500 °C) and pressure (0–50 MPa, with axial pressure and confining pressure controlled to the same value) of the core were varied to measure the deformation under diverse conditions.

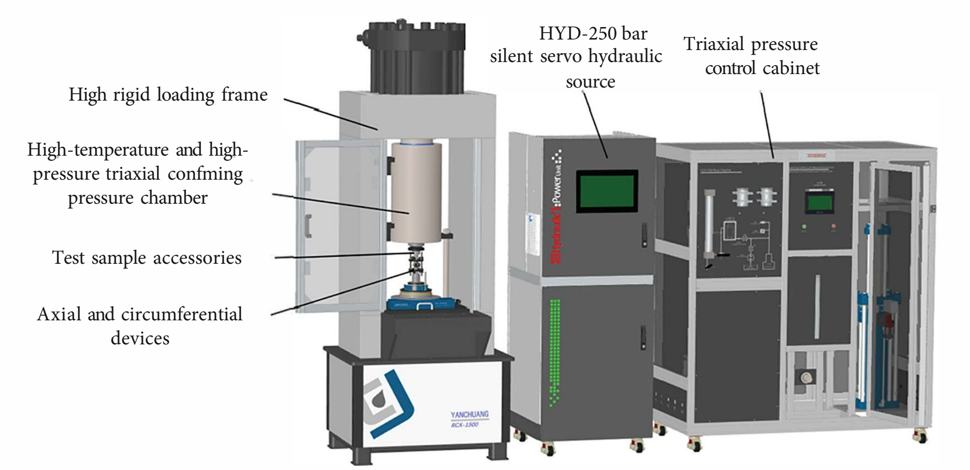

Fig. 3. RX-2000 high-temperature pseudo-triaxial rock mechanics tester.

Fig. 4. High-temperature autoclave and heat shield.

(a) (b) (c)

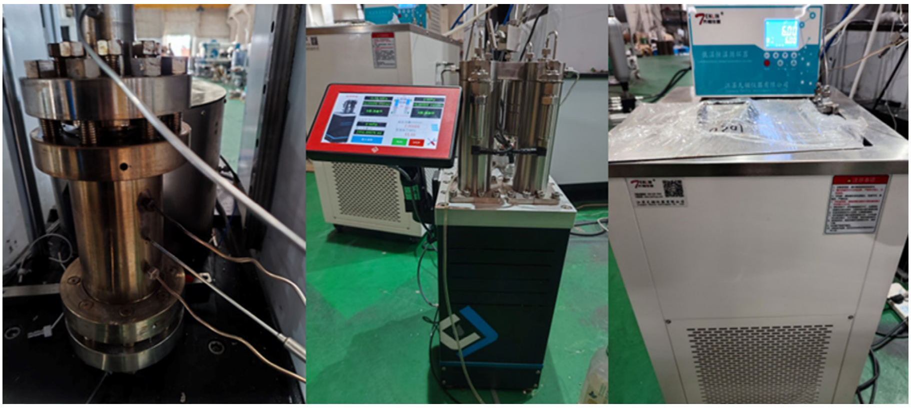

Fig. 5. Connection of high-temperature autoclave: (a) high-temperature autoclave, (b) constant pressure pumps, (c) low-temperature circulating water bath.

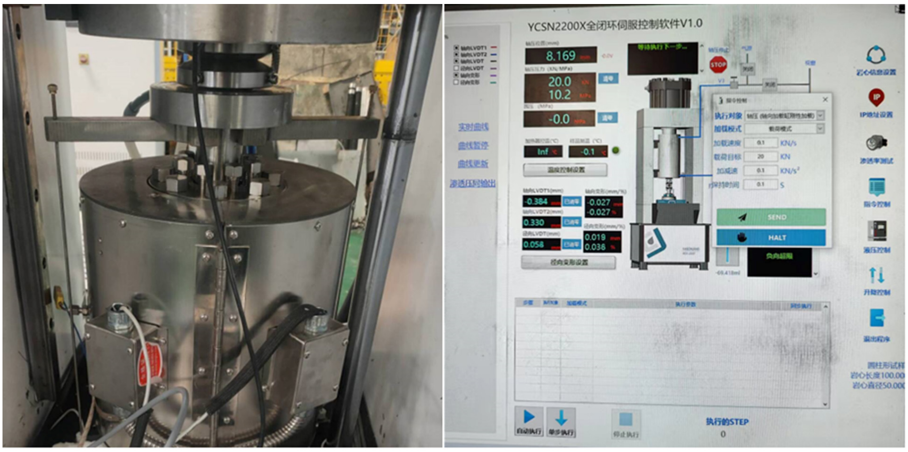

Fig. 6. Deformation monitoring device.

3. Design of deformation monitoring system for oil shale in situ heater for wells

3.1. Thermal insulation design of sensor

Given the extreme downhole temperatures of oil shale, which can reach up to 450 °C, in contrast to the significantly lower ambient temperatures encountered by the indoor experimental sensor, the sensor has been outfitted with a heat insulation device. This device is crucial for ensuring the stable and reliable operation of the oil shale in situ heater, thereby facilitating accurate and continuous monitoring of deformations under harsh conditions.

The sensor adopts a closed-loop design, featuring an Alumina 96 ceramic housing with excellent thermal insulation properties, boasting a thermal conductivity of 24 W/mK. This design enables the sensor to withstand prolonged use at temperatures up to 1000 °C, while also exhibiting remarkable corrosion resistance [34]. Furthermore, as an insulating material, it does not interfere with the normal operation of magnetic induction coils. The drive rod is crafted from UNS N06625 alloy, renowned for its exceptional fatigue resistance over a broad temperature range, from low temperatures to 1093 °C, as well as its outstanding corrosion resistance [35–37]. Internally, a vacuum chamber is constructed using 304 stainless steel for the inner layer. While 304 stainless steel possesses a high modulus of elasticity and relatively low elongation, it excels in high-temperature resistance and corrosion resistance, making it well-suited for harsh underground environments. The schematic diagram of the device is depicted in Figures 7 and 8. The magnetic induction coil is fabricated from Inconel 600, which is encapsulated within the vacuum chamber. Inconel 600 boasts remarkable resistance to high temperatures, corrosion, and stress, coupled with superior mechanical properties, ensuring stable operation under high-temperature conditions [38–41].

Given the extreme temperatures prevalent in oil shale wells, conventional signal and power transmission cables often struggle to maintain reliable operation over prolonged periods. To address this challenge, high-temperature-resistant cables have been meticulously selected for both signal transmission and heater functions. These cables exhibit remarkable pressure resilience, enduring 50 MPa at ambient temperatures and maintaining resistance of 35 MPa even at 700 °C. The core conductor of these cables comprises copper, renowned for its high melting point of 1083 °C, while the insulation layer is composed of magnesium oxide, possessing an exceptionally high melting point of 2852 °C. The construction further incorporates an inner sheath made of copper and an outer sheath of stainless steel, capable of withstanding temperatures close to its melting point of approximately 1400 °C. Designed for durability, these cables are engineered to operate continuously at temperatures exceeding 700 °C and withstand brief exposure to temperatures above 900 °C. At the heating terminal, a metal seal, fabricated from the same material as the cable body, ensures a minimum pressure resistance of 35 MPa at 700 °C, further enhancing the cable's reliability in extreme conditions.

The sensor under discussion is predominantly utilized for measuring axial deformation, prompting the design of a radial strain measurement system. As illustrated in Figure 9, two sensors are rotationally and symmetrically affixed to the sample, centered around its midpoint, and they can be effortlessly connected to the in situ heater using a snap-on mechanism. This setup ensures accurate and efficient radial strain measurements.

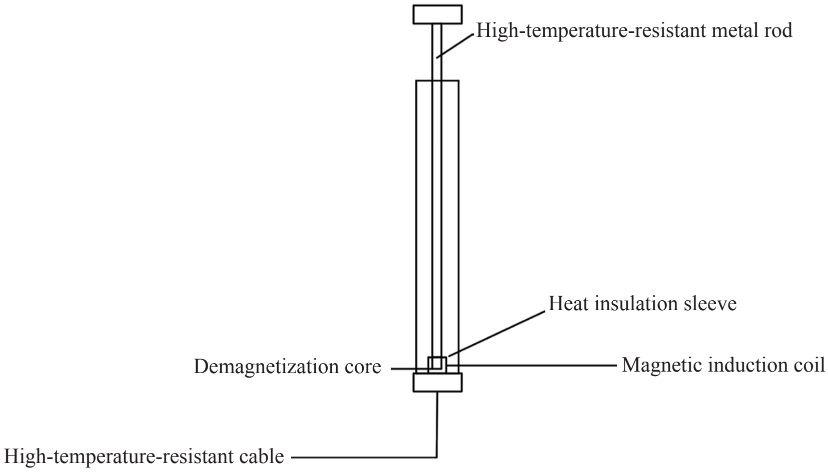

Fig. 7. Schematic diagram of sensor.

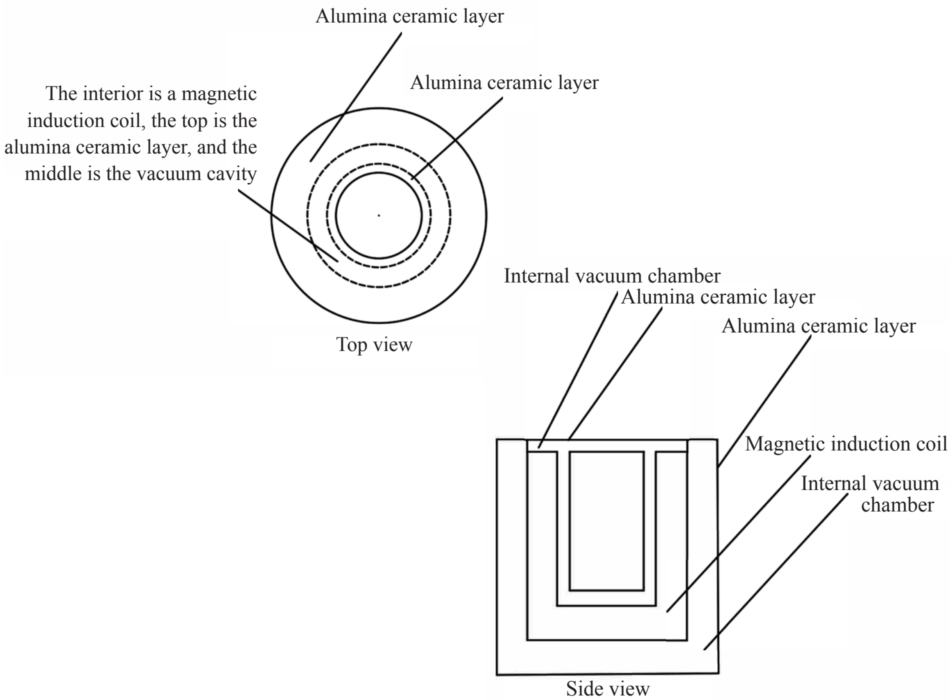

Fig. 8. Schematic diagram of heat insulation device.

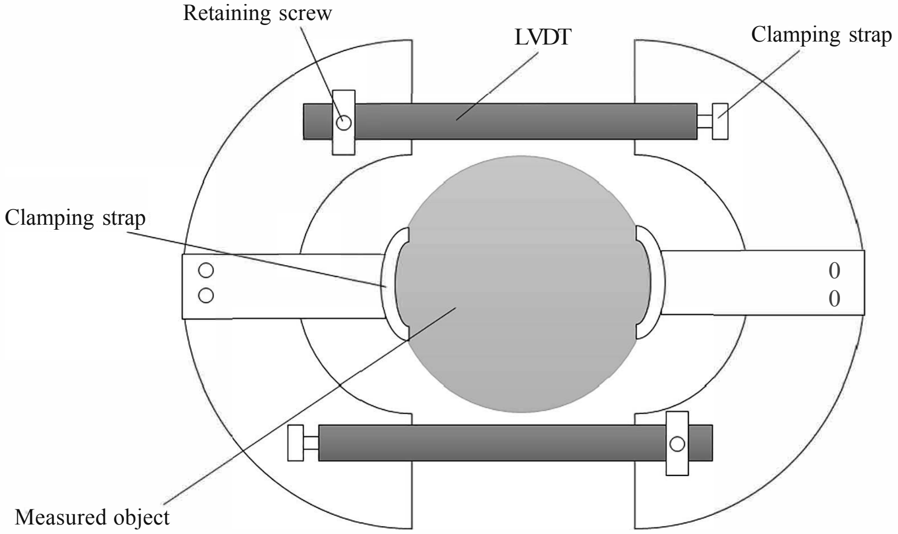

Fig. 9. Radial deformation monitoring system.

3.2. Design of deformation monitoring system for downhole deployment

Tubing deployment plays a crucial role in the downhole operations of oil wells, enabling the recording of processes involving the lifting and lowering of instruments. The tubing exhibits remarkable flexibility, allowing it to be tested in wells with diverse curvature radii, spanning from large to medium and small. Furthermore, the cable's ability to withstand pressure during descent facilitates dynamic monitoring of vertical, inclined, and horizontal wells under pressure. Therefore, this method has been selected as the optimal approach for heater deployment.

Depending on the installation position, the sensor is securely affixed to the heater via a buckle connection. Inconel 600, a material renowned for its strength and stability in high-temperature environments, has been selected as the connecting material. Before deployment, multiple LVDT sensors are strategically installed at various locations along the heater. The system is interconnected via wires, utilizing high-temperature-resistant cables as terminals for the signal transmission cables, ensuring a secure and reliable connection to each LVDT sensor.

As depicted in Figure 10, the downhole heater is securely connected to the tubing, ensuring a tight and leak-proof seal to prevent any leakage or detachment during operation. The cables of the downhole heater and deformation sensors are meticulously attached to the internal tubing cables, safeguarding them from potential damage during deployment. Subsequently, the tubing unit is initiated, and the tubing, along with the heater, is gradually lowered into the well. Throughout this process, a uniform speed is maintained

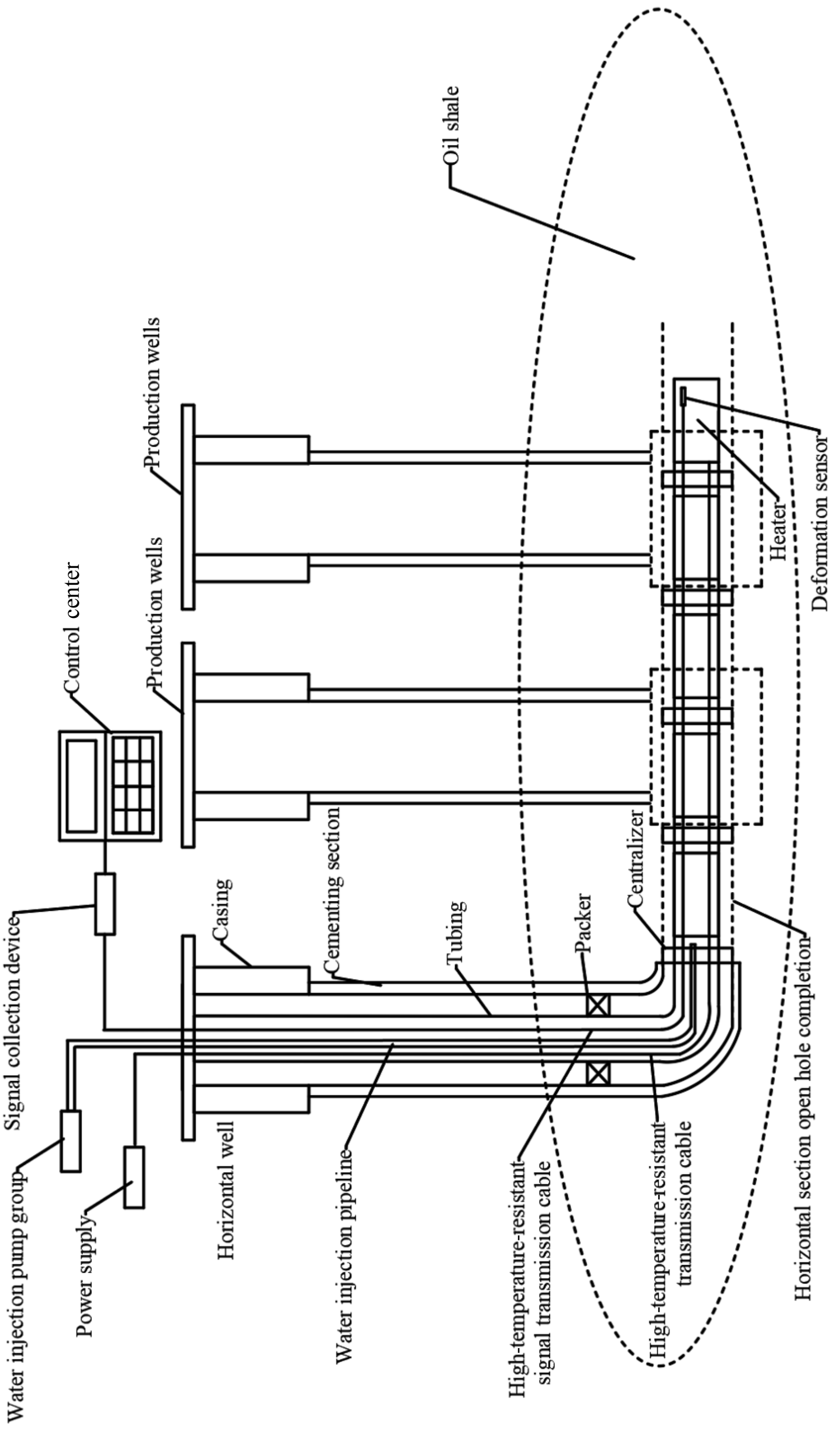

Fig. 10. Monitoring system entry mode.

to avert rapid drops or stalling, which could potentially lead to the tubing and heater becoming lodged within the wellbore. A depth gauge is employed to continually monitor the descent depth of the heater, ensuring its precise positioning at the predetermined location as planned.

Upon reaching the target location, necessary securing and plugging operations are executed to ensure that the tubing and heaters remain securely and safely positioned within the well. To accommodate downhole high-temperature and pressure conditions, packers are installed at the juncture between the horizontal and vertical sections. These packers, which are connected to the tubing, are maneuvered to the desired position and hydraulically secured within the wellbore. By pressurizing the fluid, the packer inflates and presses firmly against the well wall, sealing the annular space between the tubing and casing under high-temperature conditions. This prevents high-temperature fluids from ascending through the annulus during operation.

The packer utilizes flexible graphite, a material distinct from traditional rubber, which is extruded from expanded graphite. This material boasts excellent gas-liquid impermeability, chemical stability, resistance to both high and low temperatures, and compressive resilience. Notably, flexible graphite maintains superior physical and mechanical properties even at 450 °C, significantly outperforming materials such as polytetrafluoroethylene in terms of temperature resistance. Additionally, the packer is designed as a retrievable unit, allowing for decompression and subsequent lifting of the tubing to release both the packer and the downhole heater. The heater is fastened using a clip, facilitating easy removal of the sensor when the heater is extracted from the well's bottom.

Throughout the operation, the sensor seamlessly transmits downhole data to the control center in real-time via the signal transmission cable. Upon reaching the predetermined position, the heater initiates electric heating via the same transmission cable, ensuring efficient and timely heating as per operational requirements.

4. Experimental results and discussion

4.1. Pressure-induced deformation

As illustrated in Figure 11, under ambient temperature conditions (25 °C), the core experiences compressive deformation in response to the application of axial and confining pressures. As these pressures progressively intensify, the magnitude of deformation augments correspondingly. Conversely, Figure 12 demonstrates that under elevated temperature conditions, the continual escalation of both axial and confining pressures imposed on the core results in compressive deformation, thereby diminishing the extent of expansive deformation.

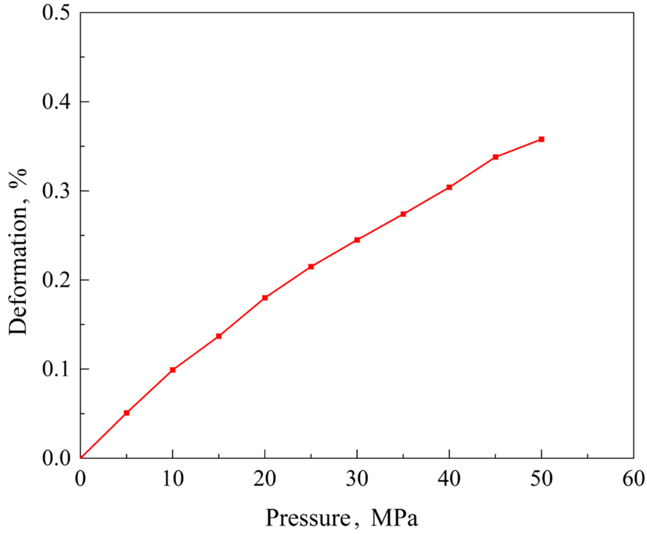

Fig. 11. Variation of deformation with pressure at room temperature.

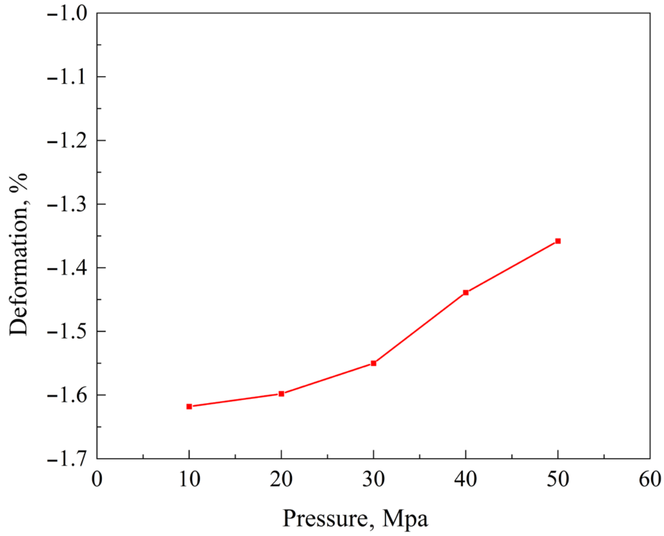

Fig. 12. Variation of deformation with pressure at 480 °C.

4.2. Temperature-induced deformation

As depicted in Figure 13, under normal pressure conditions, as the temperature of the core continuously rises, the core undergoes expansion and deformation. Notably, the magnitude of this deformation intensifies proportionately with the increase in temperature. Conversely, Figure 14 illustrates that under various constant pressure scenarios, the application of higher constant pressures leads to an augmentation in the compressive deformation experienced by the core at 25 °C. Additionally, at 480 °C, the deformation resulting from expansion gradually diminishes as the constant pressure increases.

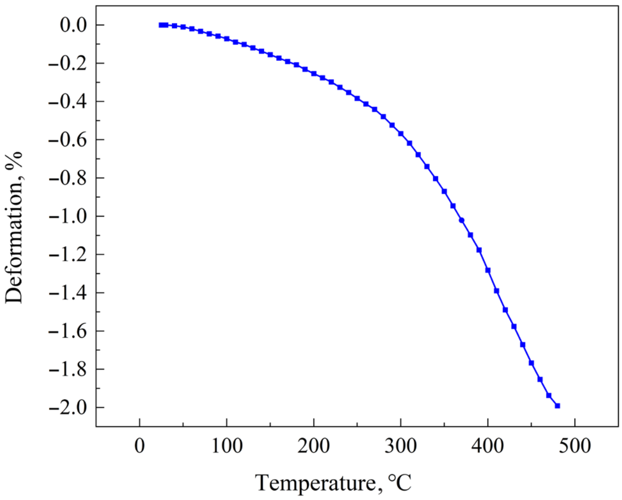

Fig. 13. Variation of deformation with temperature under atmospheric pressure.

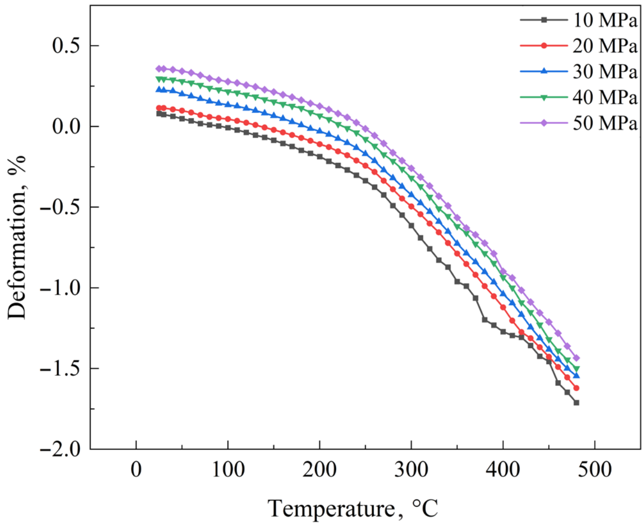

Fig. 14. Changes of deformation with temperature under different pressures.

The sensor is capable of effectively measuring deformation caused by either expansion or compression within the range of 0–50 MPa and 25–480 °C. Under the experimental conditions, temperature emerges as the primary factor contributing to deformation, with the magnitude of deformation due to expansion significantly surpassing that resulting from compression. All data for this experiment were acquired in real time through the sensor's measurements. Consequently, this sensor can be utilized for real-time monitoring of deformations in the high-temperature and high-pressure environment during the operation of oil shale downhole heaters.

5. Conclusions and prospects

5.1. Conclusions

1. This paper presents the design of a downhole deformation monitoring system for in situ heaters of oil shale, leveraging an LVDT sensor. The sensor incorporates high-temperature-resistant materials and advanced packaging techniques to guarantee stable performance even in extreme temperature environments.
2. The efficacy of the sensor has been rigorously verified through experimentation. The results demonstrate its capability to monitor deformation in real-time, withstanding temperatures ranging from 25 to 480 °C and pressures up to 50 MPa.
3. The sensor is securely connected to the heater via a buckle, with both the monitoring system and the heater conveyed to the horizontal section of the oil shale formation via tubing. To cater to the stringent requirements of high-temperature resistance within the oil shale underground environment, flexible graphite has been judiciously chosen as the packer material.

5.2. Prospects

By measuring the deformation caused by temperature under constant pressure, the temperature of an object can be deduced from the shape variable under known pressure conditions. The sensor itself has certain limitations: it necessitates a fixed reference point, and both ends of the LVDT housing should be at the same level to measure relative displacement. The heater must be securely installed before being lowered down the hole. Unlike the LVDT, fiber optic sensors do not need to be pre-fixed to the heater and can operate effectively in oil shale wells where heaters are installed. While the LVDT can be adapted for underground environments using high-temperature insulation material packaging, its overall complexity and lack of current field implementation cases make its practicality uncertain. In contrast, fiber optic sensors, which utilize high-temperature-resistant materials, can better acclimate to downhole environments, reducing the need for special packaging.

Currently, fiber optic sensors have been tested in the laboratory to measure high temperatures and high pressures, making them applicable to high-temperature and high-pressure downhole environments. However, they have yet to be used to measure the deformation of downhole heaters. Exploring non-contact relative displacement sensors, such as radar-based SEM (scanning electron microscopy) monitoring systems, PSD (position sensitive detector) sensors, and PTr (photonic transducer) sensors, is a promising research direction for accurately measuring shape variations in long rigid components.

Data availability statement

The authors confirm that the data supporting the findings of this study are available within the article.

Acknowledgments

This work was financially supported by the State Center for Research and Development of Oil Shale Exploitation, through the open fund for research on the online monitoring system for oil shale downhole heaters, and National Natural Science Foundation of China (grant No. 52274012). The authors are thankful to the reviewers and editors for their work on this article. The publication costs of this article were partially covered by the Estonian Academy of Sciences.

References

1. Sun, P., Li, W., Liu, Z., Niu, D., Wu, X., Tao, L., Wang, Z., Luan, Z. Selection of favourable targets for the in-situ conversion of continental oil shale in China. *Oil Shale*, 2023, **40**(3), 177–193. https://doi.org/10.3176/oil.2023.3.01
2. Liu, Z., Meng, Q., Dong, Q., Zhu, J., Guo, W., Ye, S., Liu, R., Jia, J. Characteristics and resource potential of oil shale in China. *Oil Shale*, 2017, **34**(1), 15–41. https://doi.org/10.3176/oil.2017.1.02
3. Xu, Y., Sun, P., Yao, S., Liu, Z., Tian, X., Li, F., Zhang, J. Progress in exploration, development and utilization of oil shale in China. *Oil Shale*, 2019, **36**(2), 285–304. https://doi.org/10.3176/oil.2019.2.03
4. Mi, S., Guo, Q., Zhang, Q., Wang, J. Classification and potential of continental shale oil resources in China and resource evaluation methods and criteria. *Oil Shale*, 2023, **40**(4), 283–320. https://doi.org/10.3176/oil.2023.4.02
5. Li, N. Y., Wang, Y., Chen, F., Han, Y. L., Chen, W., Kang, J. Development status and prospects of in-situ conversion technology in oil shale. *Spec. Oil Gas Reservoirs*, 2022, **29**(3), 1–8. https://doi.org/10.3969/j.issn.1006-6535.2022.03.001

6. Gao, C., Sun, X., Su, J., Long, Q. Global oil shale development technology and its application analysis in Xinjiang, China. *Adv. Geosci.*, 2017, **7**(3), 330–335. https://doi.org/10.12677/AG.2017.73036
7. Li, L. L., Zhang, F. Q. Current situation and suggestion of oil shale in-situ exploitation technology. C*hem. Eng.*, 2023, **37**(8), 71–75. https://doi.org/10.16247/j.cnki.23-1171/tq.20230871
8. Wang, L., Li, Z. An overview of in-situ development technology of oil shale with near and sub-critical water. *IOP Conf. Ser.: Earth Environ. Sci.*, 2019, **295**(4), 042105. https://doi.org/10.1088/1755-1315/295/4/042105
9. Hao, Y., Xiaoqiao, Q., Fansheng, X., Jialiang, Z., Yanju, L. Temperature distribution simulation and optimization design of electric heater for in-situ oil shale heating. *Oil Shale*, 2014, **31**(2), 105–120. http://dx.doi.org/10.3176/oil.2014.2.02
10. Boak, J., Kleinberg, R. Shale gas, tight oil, shale oil and hydraulic fracturing. In: *Future Energy: Improved, Sustainable and Clean Options for our Planet* (Letcher, T. M., ed.). Elsevier, Amsterdam, 2020, 67–95. https://doi.org/10.1016/B978-0-08-102886-5.00004-9
11. Hou, J., Ma, Y., Li, S., Teng, J. Development and utilization of oil shale worldwide. *Chem. Ind. Eng. Prog.*, 2015, **34**(5), 1183–1190. https://doi.org/10.16085/j.issn.1000-6613.2015.05.001
12. Tan, F., Liu, Z., Tu, J., Yu, C., Lu, C., Tam, H.-Y. Torsion sensor based on intercore mode coupling in seven-core fiber. *Opt. Express*, 2018, **26**(16), 19835–19844. https://doi.org/10.1364/OE.26.019835
13. Qi, Y., Shen, C., Wang, D., Shi, J., Jiang, X., Zhu, Z. Stacked sparse autoencoder-based deep network for fault diagnosis of rotating machinery. *IEEE Access*, 2017, **5**, 15066–15079. https://doi.org/10.1109/ACCESS.2017.2728010
14. Zhao, Z., Soto, M. A., Tang, M., Thévenaz, L. Distributed shape sensing using Brillouin scattering in multi-core fibers. *Opt. Express*, 2016, **24**(22), 25211–25223. https://doi.org/10.1364/OE.24.025211
15. Eybpoosh, M., Berges, M., Noh, H. Y. An energy-based sparse representation of ultrasonic guided-waves for online damage detection of pipelines under varying environmental and operational conditions. *Mech. Syst. Sig. Process.*, 2017, **82**, 260–278. https://doi.org/10.1016/j.ymssp.2016.05.022
16. Wang, D., Zhu, H., Zhou, G., Yu, W., Wang, B., Zhou, W. Monitoring shear deformation of sliding zone via fiber Bragg grating and particle image velocimetry. *J. Rock Mech. Geotech. Eng.*, 2024, **16**(1), 231–241. https://doi.org/10.1016/j.jrmge.2023.03.007
17. Xin, W., Pu, C., Liu, W., Liu, K. Landslide surface horizontal displacement monitoring based on image recognition technology and computer vision. *Geomorphology*, 2023, **431**, 108691. https://doi.org/10.1016/j.geomorph.2023.108691
18. Yue, Z., Huang, L., Lin, Y., Lei, M. Research on image deformation monitoring algorithm based on binocular vision. *Measurement*, 2024, **228**, 114394. https://doi.org/10.1016/j.measurement.2024.114394

19. Chen, X., Xu, N., Yang, L., Xiang, D. High temperature displacement and strain measurement using a monochromatic light illuminated stereo digital image correlation system. *Meas. Sci. Technol.*, 2012, **23**(12), 125603. https://doi.org/10.1088/0957-0233/23/12/125603
20. Berke, R. B., Lambros, J. Ultraviolet digital image correlation (UV-DIC) for high temperature applications. *Rev. Sci. Instrum.*, 2014, **85**(4), 045121. https://doi.org/10.1063/1.4871991
21. Qiao, M. X., Pan, Z. W., Huang, S. H., Su, Y., Zhang, Q. C. Investigation on digital image correlation measurement technique for high temperature deformation of tungsten materials in vacuum environment. *J. Exp. Mech.*, 2020, **35**(4), 557–566. https://doi.org/10.7520/1001-4888-19-066
22. Xia, P., Tan, Y., Li, T., Zhou, Z., Lv, W. A high-temperature resistant photonic crystal fiber sensor with single-side sliding Fabry-Perot cavity for super-large strain measurement. *Sens. Actuators A: Phys.*, 2021, **318**, 112492. https://doi.org/10.1016/j.sna.2020.112492
23. Li, C. H., Song, Z. Q., Zhang, B., Yang, S. H., Wu, W. X. An all-fiber Fabry-Perot type high-temperature strain sensor. *Struct. Environ. Eng.*, 2024, **51**(3), 60–64. https://doi.org/10.19447/j.cnki.11-1773/v.2024.03.008
24. Gao, H. C., Tang, C. J., Lan, T., Wang, X. F. Research progress of high temperature fiber Fabry-Perot pressure sensor. *Instrum. Tech. Sens.*, 2020, **57**(12), 26–31.
25. Yu, Q. X., Wang, X. N., Song, S. D., Zhao, Y. W., Cui, S. B. Fiber optic pressure sensor system based on extrinsic Fabry-Perot interferometer for high temperature oil well measurement. *J. Optoelectron. Laser*, 2007, **18**(3), 299–302.
26. Li, S. X., Ma, L., Lü, J. S., Zhang, F. X., Liu, X. H., Zhao, Q. C., Li, H., Wang, C. Design of high precision fiber Bragg grating temperature sensor for rapid measurement of oil well temperature profile. *Shandong Sci.*, 2018, **31**(3), 55–60. https://doi.org/10.19447/j.cnki.11-1773/v.2024.03.008
27. Yang, B., Zhao, Q. C., Che, C. R., An, B. X., Xu, Z. High-precision optical fiber temperature and pressure sensor and its application in production wells. *Laser Optoelectron. Prog.*, 2022, **59**(17), 128–133. https://doi.org/10.3788/LOP202259.1706006
28. Wang, G. *Research on Monitoring Technology of Casing Deformation in Oil and Water Well Based on Optical Fiber Sensing*. Master's thesis. Qilu University of Technology, 2021.
29. Chen, W. B., Feng, W. Q., Yin, J. H., Borana, L. LVDTs-based radial strain measurement system for static and cyclic behavior of geomaterials. *Measurement*, 2020, **155**, 107526. https://doi.org/10.1016/j.measurement.2020.107526
30. Mayunga, S. D., Bakaone, M. Dynamic deformation monitoring of Lotsane bridge using global positioning systems (GPS) and linear variable differential transducers (LVDT). J. *Data Anal. Inf. Process.*, 2021, **9**(1), 30–50. https://doi.org/10.4236/jdaip.2021.91003
31. Gruber, G., Neumayer, M., Schweighofer, B., Wegleiter, H. Linear variable differential transformer in harsh environments – analysis of temperature drifts

for different plunger materials. *IEEE Sens. Lett.*, 2023, **7**(9), 1–4. https://doi.org/10.1109/LSENS.2023.3306981
32. Li, S., Yu, Y., Duan, C. Analysis of influence of temperature on performance index of LVDT sensor. *Electron. Commun. Comput. Sci.*, 2024, **6**(4), 52–54. https://doi.org/10.37155/2717-5170-0604-18
33. Petchmaneelumka, W., Rerkratn, A., Luangpol, A., Riewruja, V. Compensation of temperature effect for LVDT transducer. *J. Circuits Syst. Comput.*, 2018, **27**(12), 1850182. https://doi.org/10.1142/S0218126618501827
34. Ghosh, S., Sengupta, A., Pal, K. S., Dandapat, N., Chakraborty, R., Datta, S., Basu, D. Characterization of metallized alumina ceramics. *Metall. Mater. Trans. A*, 2012, **43**(3), 912–920.
35. Delblanc, A., Mattsson, R., Gullberg, D., Eidhagen, J. Investigation of the crevice corrosion resistance of UNS S31266 and UNS N06625 using accelerated laboratory test methods. In: *CORROSION 2019 Conference & Expo*, March 24–28, 2019, Nashville, Tennessee. NACE International, 2019, NACE-2019-13077.
36. Thorhallsson, A. I., Stefansson, A., Karlsdottir, S. N. Corrosion testing of UNS N06625 in a simulated high temperature geothermal environment. In: *CORROSION 2018 Conference & Expo*, April 15–19, 2018, Phoenix, Arizona. NACE International, 2018, NACE-2018-11058.
37. Zhang, C. L., Wang, X. P., Ning, T. X., Chen, S. C., Luo, L. Y. Simulation test and analysis on hot forming process of alloy UNS N06625. *Spec. Steel*, 2017, **38**(2), 1–5.
38. Abels, J.-M., Strehblow, H.-H. A surface analytical approach to the high temperature chlorination behaviour of Inconel 600 at 700 °C. *Corros. Sci.*, 1997, **39**(1), 115–132. https://doi.org/10.1016/S0010-938X(96)00112-6
39. Herrera-Chávez, L. Y., Ruiz, A., López-Morelos, V. H., Rubio-González, C. Microstructural characterization and mechanical response of Inconel 600 welded joint. *Mater. Charact.*, 2019, **157**, 109882. https://doi.org/10.1016/j.matchar.2019.109882
40. Karthik, D., Swaroop, S. Laser shock peening enhanced corrosion properties in a nickel based Inconel 600 superalloy. *J. Alloys Compd.*, 2017, **694**, 1309–1319.
41. Shapiro, E., Dieter, G. E. High temperature-high strain rate fracture of Inconel 600. *Metall. Trans.*, 1970, **1**(6), 1711–1719.